academicJournals

Vol. 16(32), pp. 1705-1716, 9 August, 2017
DOI: 10.5897/AJB2017.16010
Article Number: 92204D865694
ISSN 1684-5315

http://www.academicjournals.org/AJB

African Journal of Biotechnology

Full Length Research Paper

Antibacterial and antioxidant activity of silver nanoparticles synthesized using aqueous extract of *Moringa stenopetala* leaves

Abambagade Abera Mitiku[1*] and Belete Yilma[2]

[1]Department of Chemistry, Arba Minch College of Teachers Education, Southern Nations, Nationalities and Peoples' Region, Ethiopia.
[2]Department of Chemistry, College of Natural Sciences, Arba Minch University, Southern Nations, Nationalities and Peoples' Region, Ethiopia.

Received 29 March, 2017; Accepted 31 July, 2017

Green synthesis of silver nanoparticles (AgNPs) is non-toxic and eco-friendly than commonly used physicochemical methods. The study focuses on synthesis, characterization, antibacterial and antioxidant activity of AgNPs synthesized using aqueous extract of *Moringa stenopetala (M. stenopetala)* leaves. Optimum heating time required for the preparation of aqueous extract of *M. stenopetala* leaves was 15 min. It was found that 90 ml of 1 mM of silver nitrate solution and 15 ml of aqueous extract of *M. stenopetala* leaves were more favorable for maximum production of AgNPs with a yield of 97.14%. Ultraviolet-visible (UV-Vis) spectrum of synthesized AgNPs shows a peak at 412 nm. Fourier transform infrared spectroscopy (FTIR) spectral analysis indicated involvement of -C=O, -O-H, and -N-H in the formation of AgNPs. X-ray diffraction (XRD) pattern showed the face centered cubic (FCC) structure of AgNPs with average particle size of 11.44 nm. Synthesized AgNPs showed stronger antibacterial activity against *Escherichia coli* than *Staphylococcus aureus* and has better antioxidant activity than standard ascorbic acid.

Key words: Silver nanoparticles (AgNPs), green synthesis, *Moringa stenopetala*.

INTRODUCTION

Nanotechnology is a broad field of science that represents the design, synthesis, characterization and application of materials at nanoscale level which can be used across various fields such as chemistry, biology, physics, material science, medicine, etc. (Surya et al., 2016; Jassim et al., 2016) and nanoparticles (NPs) are viewed as fundamental building blocks of nanotechnology (Vastrad and Goudar, 2016). The term “nanoscale” is generally referred to a scale between 1 and 100 nm (Lakshman et al., 2016).

Green synthesis of silver nanoparticles (AgNPs) provides advancement over physicochemical methods as it is cost effective, eco-friendly, easily scaled up and there is no need to use high energy, temperature and toxic chemicals (Sadeenp et al., 2016).

Moringa is a tropical plant belonging to the family

*Corresponding author. E-mail: evachemistry@gmail.com.

Figure 1. *Moringa stenopetala* plant.

Moringaceae. Among the different species, *Moringa oleifera* and *Moringa stenopetala* are the most widely known and utilized species of Moringa plant. Based on the multipurpose behavior of Moringa several impressive bynames has been given such as “The Tree of Life”, “The Never Die Tree”, “The Magic Tree”, “The Tree of Paradise”, and “Mothers' Best Friend”. *Moringa stenopetala* is often referred to as the East African Moringa tree because it is native only to southern Ethiopia and northern Kenya (Kekuda et al., 2016). *M. stenopetala* tree has both nutritional and medicinal values (Raghavendra et al., 2016). Nowadays, plant extract has been used as reducing and capping agent for the synthesis of AgNPs. Many natural biomolecules in plants (inactivated plant tissue, plant extracts and living plant) such as proteins/enzymes, amino acids, polysaccharides, alkaloids, alcoholic compounds, and vitamins involved in bioreduction, formation and stabilization of AgNPs (Abeer, 2016) .The reducing property of *M. stenopetala* plant constituents plays a critical role in the reduction of Ag^{+} ions to AgNPs and stabilization of AgNPs.

The antimicrobial and multi-drug resistance (MDR) of human pathogens made as problematic issue which needs to discover new natural alternates to overcome this problem (Pak et al., 2016). AgNPs seem to be alternative antibacterial agents to antibiotics and have the ability to overcome the bacterial resistance against antibiotics. Therefore, it is necessary to develop AgNPs as antibacterial agents. Among the several promising nanomaterials, AgNPs seem to be potential antibacterial agents due to their large surface-to-volume ratios and crystallographic surface structure (Zhang et al., 2016). Free radicals are produced in normal and/or pathological cell metabolism. However, uncontrolled productions of oxygen derived free radicals are involved in the onset of many diseases. Antioxidants provide chemical protection for biological systems against harmful effects of reaction that are excessive oxidation, protein damage, DNA damage and cell death (Priyanka et al., 2016).

To the best of our knowledge, there is no work reported on synthesis, characterization, antibacterial and antioxidant activities of AgNPs synthesized using extract of *M. stenopetala* plant. The objective of the current study was to develop a simple, non-toxic, cost effective and eco-friendly approach for the synthesis of AgNPs using aqueous extract of *M. stenopetala* leaves and characterization of synthesized AgNPs using visual observation, ultraviolet-visible (UV-Vis), Fourier transform infrared spectroscopy (FTIR) and x-ray diffraction (XRD). Further, antibacterial activity of synthesized AgNPs was analyzed against *Staphylococcus aureus* and *Escherichia coli* bacteria. The *in vitro* hydrogen peroxide scavenging potential of synthesized AgNPs using ascorbic acid as standard was also evaluated.

MATERIALS AND METHODS

Collection and identification of *M. stenopetala* leaves

Fresh leaves of *M. stenopetala* were collected in October 2015 from Southern part of Ethiopia, Konso district. *M. stenopetala* plant (Figure 1) was botanically identified using the standard morphological characteristic features. The tree was already confirmed and labelled on the tree as per information and authenticated by a taxonomist.

Preparation of *M. stenopetala* leaves powder and aqueous extract

The fresh leaves of *M. stenopetala* were dried under shade at room temperature for 11 days. The shade dried leaves of *M. stenopetala* were ground to form powder using a mortar and pestle (Raghasudha, 2016). The powdered leaves of *M. stenopetala* were stored in well labeled airtight container.

Twenty grams of powdered leaves were weighed using electronic balance (OHASUS E11140) and transferred into 500 ml beaker containing 100 ml of distilled deionized water. The mixture was

heated on hot plate for 15 min at 60°C, allowed to cool and filtered through Whatman No.1 filter paper. Freshly prepared aqueous extract of *M. stenopetala* leaves were stored at 4°C for further use as a reducing, capping and stabilizing agent for the synthesis of AgNPs without further treatment (Kumar et al., 2015).

Preparation of 1 mM of silver nitrate solution

Seventeen milligrams (17 mg) of silver nitrate (Blulx laboratories (P) Ltd. 99.9% $AgNO_3$, MW = 169.87 g/mol) were weighed using electronic balance and transferred into 500 ml Erlenmeyer flask. The silver nitrate was slowly dissolved by gently swirling the flask containing distilled deionized water. After all the solid has dissolved, more water was slowly added to bring the level of solution exactly to a volume mark of 100 ml. The prepared 1 mM silver nitrate solution was stored at 4°C in amber colored bottle (Malathi and Rajkumar, 2015).

Synthesis of silver nanoparticles

A volume of 15 ml of aqueous extract of *M. stenopetala* leaves was added to 90 ml of 1 mM of silver nitrate solution in 500 ml Erlenmeyer flask for reduction of Ag^+ ions and stabilization of AgNPs (Thampi and Jeyadoss, 2015a).

Optimization of synthesis parameters

Heating time of *M. stenopetala* leaves at 60°C (5, 10, 15, 20, 25 and 30 min), concentration of silver nitrate solution (0.25, 0.5, 0.75, 1 and 1.25 mM), volume of 1 mM of silver nitrate solution (10, 30, 60, 90 and 120 ml) and volume of aqueous extract of *M. stenopetala* leaves (5, 10, 15, 20 and 25 ml) were investigated by varying the parameters one at a time at room temperature.

Determination of yield of prepared silver nanoparticles using atomic absorption spectroscopy (AAS)

Reaction mixture was centrifuged at 110 × 100 rpm for 10, 20 and 30 min after 24 h of incubation time. Amount of unreacted Ag^+ ions and percentage yield of AgNPs is calculated based on initial concentration Ag^+ ions (Devadiga et al., 2015).

$$\text{Total yield} = \frac{\text{initial } \left[Ag^+\right] \text{ions in ppm} - \text{final } \left[Ag^+\right] \text{ions in ppm}}{\text{initial } \left[Ag^+\right] \text{ions in ppm}} \text{x100}$$

Separation and purification of silver nanoparticles

After desired reaction period, the mixture containing product was centrifuged (Rotant 98, Hettich, Ze ntrifugen, UK) at 110 × 100 rpm for 20 min. The process of centrifugation and re-dispersion in distilled deionized water was repeated three times to ensure better removal of unreacted phytochemicals from the AgNPs (Premasudha et al., 2015).

Characterization of silver nanoparticles

Visual observation

The colour change in reaction mixture was recorded through visual observation.

UV-Vis measurements

Bioreduction of Ag^+ ions were monitored by measuring the UV-Vis (SANYO SP65) spectra of the reaction mixture at a resolution of 1 nm in the range of 200 to 800 nm (Ahmed et al., 2015).

FTIR measurements

FTIR (Perkin Elmer, spectrum 65) spectral analysis was carried out to identify biomolecules responsible for the reduction of Ag^+ ions and stabilization of AgNPs (Saminathan, 2015). Dried sample of the product was ground with KBr pellets and analyzed using FTIR spectroscopy operating at a resolution of 4 cm^{-1} in the region of 4500 to 400 cm^{-1}.

XRD measurements

The crystallite size of synthesized product was determined using X-ray diffractometer (D8 Advanced BRUKER AXS GmbH, Germany) operating at a voltage of 40 kV and a current of 30 mA with CuKα radiation operating between 10 and 80° of 2θ angles at scanning rate of 2° per min.

Antibacterial activity of silver nanoparticles

Antibacterial activity of test samples was determined against *S. aureus* and *E. coli* as test micro-organisms, using agar well diffusion assay method. Muller Hinton Agar (Hi-Media Lab. Pvt. Ltd., India) was prepared, poured in sterile petri dishes and allowed to solidify (Gopalakrishnan et al., 2016). A strain of *S. aureus* and *E. coli* was swabbed uniformly on individual plates using sterile cotton swab. Holes were made in each plate with the help of sterilized stainless steel cork borer. Each hole was filled with 14 µl of different concentrations (25, 50, 75 and 100 µg/ml) of test samples using micropipette. All the Petri dish plates containing micro-organism and test samples were incubated at 37°C for 24 h at room temperature. The diameter of zone of inhibition was measured in millimeter around each well using a ruler.

Antioxidant activity of silver nanoparticles

The ability of AgNPs to scavenge hydrogen peroxide (30% H_2O_2, Image chemicals) was determined by standard method (Thampi and Shalini, 2015b). A solution of hydrogen peroxide (40 mM) was prepared in phosphate buffer saline (pH=7.4). Different concentrations of test samples (10, 20, 30, 40 and 50 µg/ml) were prepared, from each concentration 4 ml of test sample was mixed with 0.6 ml of previously prepared H_2O_2 solution. Absorbance of solution was measured at 230 nm after 10 min against blank solution using UV-Vis spectrophotometer.

RESULTS AND DISCUSSION

Optimization of synthesis parameters

Heating time of extract

Maximum absorbance of the synthesized AgNPs increased gradually with increase in heating time of *M. stenopetala* leaves from 5 min up to 15 min at 60°C and began to decline until it reached 30 min (Figure 2a).

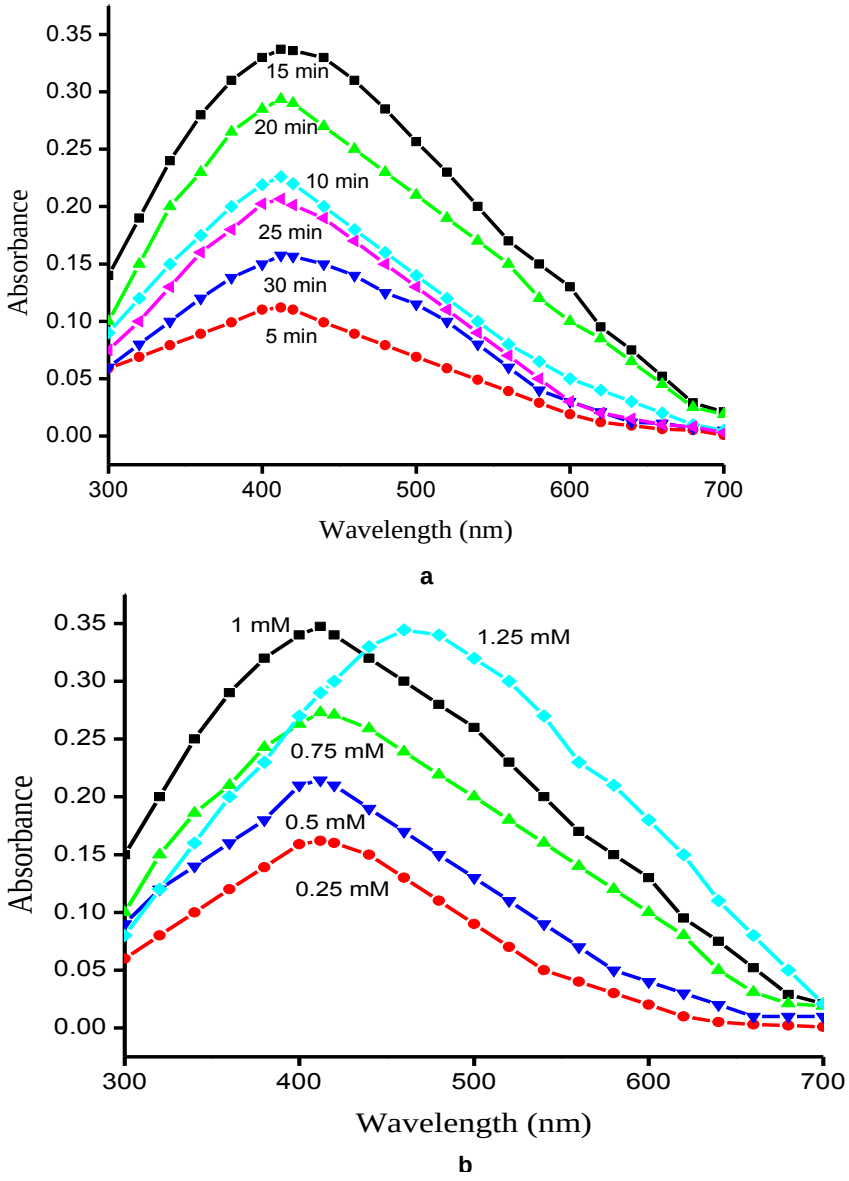

Figure 2. (a) Absorption spectra of AgNPs with varying extract heating time. **(b)** Absorption spectra of AgNPs with varying silver nitrate concentration as prepared.

When the heating time of extract was more than 15 min, there was a decrease in maximum absorbance of AgNPs; higher heating time degraded the phytochemicals present in the *M. stenopetala* leaves. The present study indicates that the optimal heating time required for the preparation of aqueous extract of *M. stenopetala* leaves was 15 min.

Silver nitrate concentration

As shown in Figure 2b, the highest peak was attained at a wavelength of 412 nm (λ_{max} = 412 nm) with the solution of 1 mM silver nitrate prepared. Also, from the UV-Vis spectra (Figure 2b), it was observed that with increase in the concentration of silver nitrate from 0.25 to 1 mM, maximum absorbance of AgNPs increased. However, further increase in the concentration of silver nitrate led to a decrease in maximum absorbance value and shifting of SPR peak to a longer wavelength (Figure 2b), a red shift (λ_{max} = 460 nm) which causes aggregation and agglomeration of the synthesized AgNPs.

Volume of silver nitrate solution

The study shows that as the volume of 1 mM of silver nitrate solution increases from 10 to 90 ml, maximum absorbance of AgNPs increases (Figure 3a). For 90 ml of

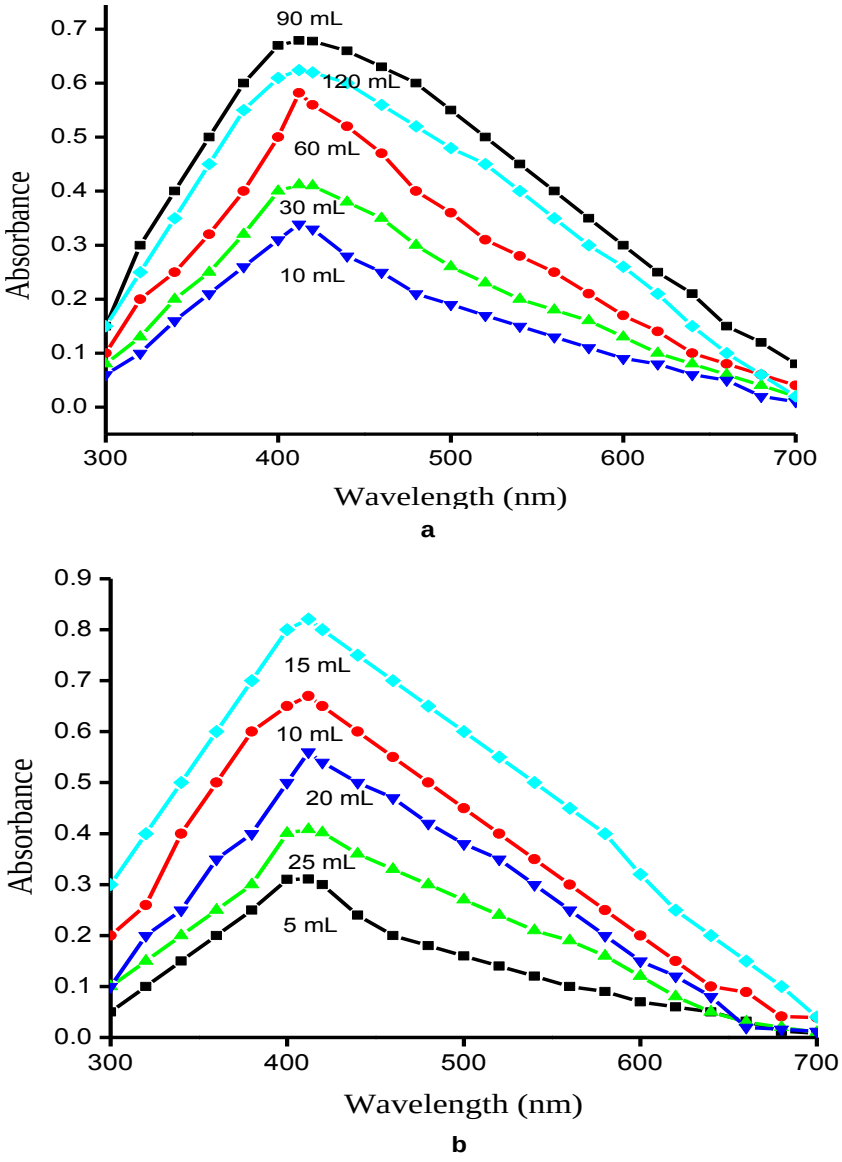

Figure 3. (a) Absorption spectra of AgNPs with varying volume of 1 mM of silver nitrate solution; (b) Absorption spectra of AgNPs with varying volume of aqueous extract of *M. stenopetala* leaves as prepared.

silver nitrate solution, the maximum absorbance (Figure 3a) indicated the complete reduction of Ag^+ ions to AgNPs. However, further increase in volume of 1 mM of silver nitrate led to decrease in maximum absorbance value (Figure 3a).

Volume of aqueous extract of M. stenopetala leaves

UV-Vis spectra (Figure 3b) show increase in maximum absorbance of AgNPs with increase in volume of aqueous extract of *M. stenopetala* leaves from 5 to 15 ml. When the volume of aqueous extract of *M. stenopetala* leaves is more than 15 ml, there is a decrease in maximum absorbance of AgNPs, due to the binding of more phytochemicals on the surface of AgNPs. Moreover, at higher extract concentration intensity of absorption decreases and the solution becomes hazy due to the presence of excess biomolecules (Parveen et al., 2016).

Characterization of silver nanoparticles

Visual observation

The formation of AgNPs was primarily observed by colour change of the aqueous extract of *M. stenopetala* leaves

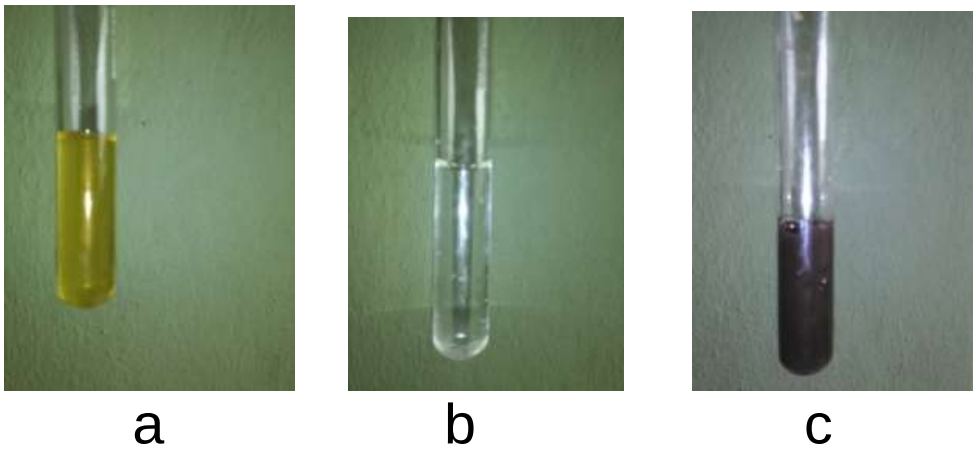

Figure 4. (a) Color of aqueous extract of *M. stenopetela* leaves. **(b)** Silver nitrate solution. **(c)** Silver nitrate with aqueous extract of *M. stenopetala* leaves.

(yellowish green colour; Figure 4a) after treatment with silver nitrate (colorless solution; Figure 4b) to dark brown for AgNPs (Figure 4c).

The colour of silver nitrate solution changed from colorless to dark brown upon addition of leaf extract, indicating the formation of AgNPs was also reported in the literature (Sultana et al., 2015).

UV-Vis spectral analysis

The highest peak that is observed at 412 nm (Figure 5a) corresponds to surface plasmon resonance (SPR) and indicates formation of AgNPs. AgNPs have free electrons, which give SPR absorption band, due to the combined vibration of electrons of AgNPs in resonance with light wave (Balashanmugam and Kalaichelvan, 2015). In the present study, a single SPR band is exhibited, which shows no agglomeration of AgNPs.

From Figure 5b, it is noted that absorbance of AgNPs increases with time as increasing the incubation time up to 24 h. Above 24 h of reaction time; there is no significant change in the absorbance, which indicates the maximum attainability in the stability of the AgNPs. There is no obvious change in colour intensity, spectral peak position and absorbance of AgNPs, when monitored at regular intervals over a period of 6 months.

FTIR spectral analysis

The FTIR spectrum of aqueous extract of *M. stenopetala* leaves (Figure 6a) shows the presence of different peaks. The strong peak at 3434 cm^{-1} in the FTIR spectrum indicates N–H stretching vibration of amino groups and -OH stretching of hydroxyl group in phenols (Hassan et al., 2016). A peak observed at 2,922 cm^{-1} is due to C-H stretching of alkane amide I band of proteins (Selvam and Sivakumar, 2015). The peak at 1639.5 cm^{-1} corresponds to amine groups of–N–H bending vibrations of proteins and characteristic of -C=O carbonyl groups (Selvam and Sivakumar, 2015). A peak at 2851.5 cm^{-1} belongs to the C-H stretching vibration of $-CH_3$ and $-CH_2$ groups (Wojtan et al., 2016). The peak at 1739 cm^{-1} corresponds to -C=O stretching of carbonyl group in ketones, aldehydes and carboxylic acid (Nagaonkar and Rai, 2015). The peak at 1384.5 cm^{-1} corresponds to bending vibrations of -OH or C-N stretching of aromatic amine (Bonigala et al., 2016). The peak at 1060 cm^{-1} corresponds to C-O stretching from alcohol, carboxylic acid, and C-N stretching vibration of amine.

The FTIR spectrum of biosynthesized AgNPs (Figure 6b) shows the presence of different peaks. The peak at 3426 cm^{-1} in the FTIR spectrum indicates O-H group in alcohols, phenols and N-H stretching vibration of amides of protein. The peak at 2920.5 and 2850 cm^{-1} corresponds to aliphatic CH, CH_2, and CH_3 groups. The peak at 1745 cm^{-1} corresponds to C=O stretching and N-H bending in amides (Fasasi et al., 2015). The peak at 1601.5 cm^{-1} corresponds to C=C in ring system or double bond stretching in C=O and C=N. The sharp peak at 1384.5 cm^{-1} corresponds to C-N stretching of aromatic amine group or secondary amines. The peak at 1031 cm^{-1} corresponds to C-O stretching of alcohols, carboxylic acids, or C-N stretching of aliphatic amines (Basker, 2016).

FTIR studies confirm that the carbonyl groups from the amino acid residues and proteins have the stronger ability to bind AgNPs to prevent agglomeration and thereby stabilize the AgNPs through free amine groups in proteins (Sangeetha et al., 2016).

XRD analysis

Miller indices (hkl) are necessary to be assigned for each

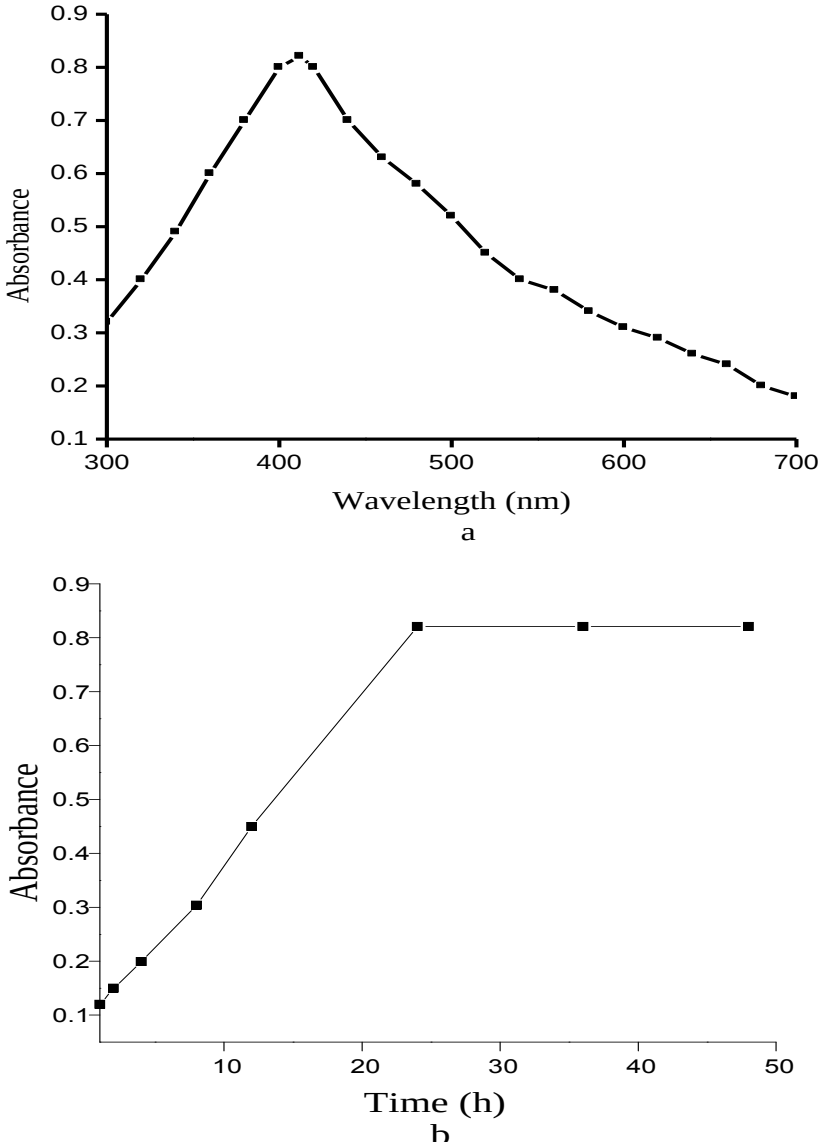

Figure 5. (a) UV-Vis absorption spectrum of AgNPs synthesized using aqueous extract of *M. stenopetala* leaves (15 ml of extract was added in to 90 ml of 1 mM of $AgNO_3$) at room temperature. **(b)** Absorbance recorded as function of incubation time for AgNPs as prepared.

peak to index. The distinct diffraction peaks at 37.74, 44.04, 64.2 and 77.26° corresponds to 111, 200, 220 and 311 facets of the face centered cubic (FCC) crystal structure, respectively (Table 1). A typical XRD pattern of the synthesized AgNPs using aqueous extract of *M. stenopetala* leaves is found to possess a FCC structure, which go very well with the values manipulated for FCC structure of silver nano-crystals (Joint Committee on Powder Diffraction Standards: File No. 04-0783) (Bykkam et al., 2015).The average particle size of synthesized AgNPs is calculated from FWHM of the diffraction peaks using Debye-Scherrer equation (Bykkam et al., 2015) (Figure 7).

$$D = \frac{0.9\lambda}{\beta Cos\theta}$$

Where, "D" is particle diameter size, λ is wave length of X-ray (0.1541 nm), β is FWHM, and θ is the diffraction angle.

The value of d (the interplanar spacing between the atoms) is calculated using Bragg's Law.

$$d = \frac{\lambda}{2xSin\theta}$$; λ = 0.1541 nm for CuKα.

The average particle size of biosynthesized AgNPs in

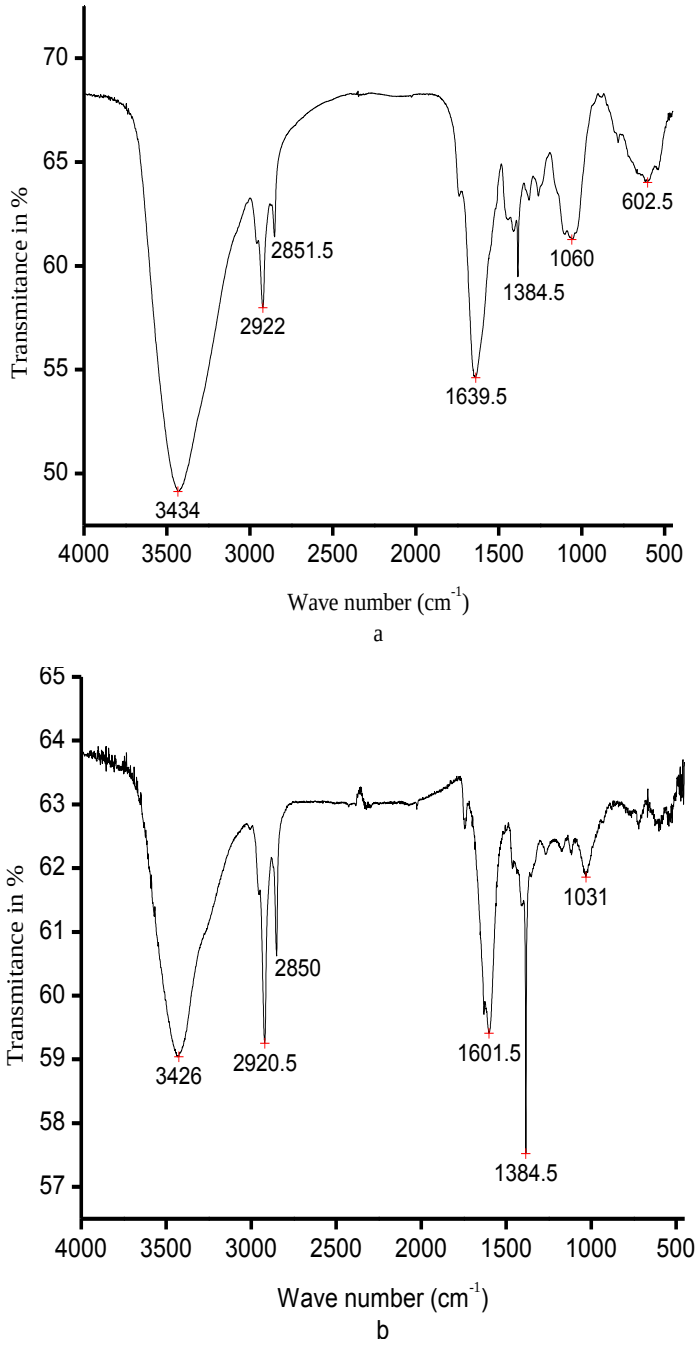

Figure 6. (a) FTIR spectrum of aqueous extract of *M. stenopetala* leaves. **(b)** FTIR spectrum of AgNPs synthesized at room temperature as prepared.

Table 1. Peak indexing from d-spacing.

Peak position 2θ	d	d^2	$1000/d^2$	$(1000/d^2)/60.53$	hkl	Remarks
37.74	2.382	5.673	176.27	3	111	$1^2+1^2+1^2=3$
44.04	2.055	4.223	236.80	4	200	$2^2+0^2+0^2=4$
64.2	1.450	2.102	475.74	8	220	$2^2+2^2+0^2=8$
77.26	1.234	1.523	655.6	11	311	$3^2+1^2+1^2=11$

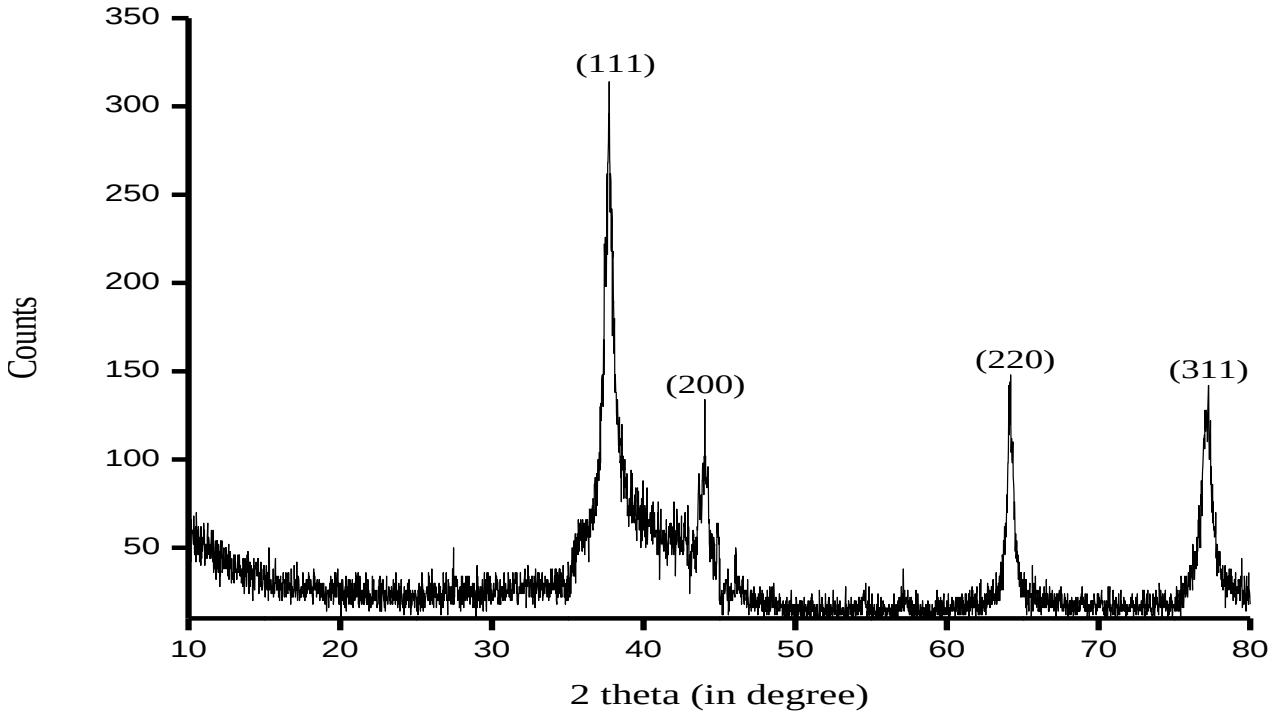

Figure 7. XRD pattern of AgNPs synthesized at room temperature as prepared.

present study is 11.44 nm as prepared.

Determination of yield of silver nanoparticles using atomic absorption spectroscopy (AAS)

AAS analysis was carried out to analyze unreacted Ag^+ ion concentration, which shows the conversion of Ag^+ ions into AgNPs (Choudhary et al., 2016).

The conversion of Ag^+ to AgNPs and percentage yield of AgNPs increases with increasing centrifugation time. From the point of view of time and energy, 20 min of centrifugation time is selected. In the present study, it is comparatively high yield of AgNPs (97.14%) and took about 20 min of centrifugation which is quite more than yield of AgNPs (87%) reported in the literature (Mehmood et al., 2016).

Antibacterial activity of silver nanoparticles

Experimental results are expressed as mean ± standard deviation (SD). Biosynthesized AgNPs shows the highest antibacterial activity against *E. coli* (38.00± 0.61 mm, Figure 8a) in 100 µg/ml and the lowest antibacterial activity against *S. aureus* (11.00± 0.41 mm, Figure 8a) in 25 µg/ml. Silver nitrate solution shows the highest antibacterial activity against *E. coli* (28.00±0.41 mm, Figure 8b) in 100 µg/ml and the lowest antibacterial activity against *S. aureus* (9.00 ± 0.58 mm, Figure 8b) in 25 µg/ml. When antibacterial activity of silver nitrate and AgNPs are compared against the studied bacteria, an increase in antibacterial activity of AgNPs over the use of silver nitrate is observed. Similarly, it has been reported that AgNPs show higher antibacterial activity than silver nitrate (Marslin et al., 2015).

The high surface area to volume ratio of AgNPs increases their contact with micro-organisms, promoting the dissolution of Ag^+ ions and hence improving biocidal effectiveness. Formation of free radicals by the AgNPs when in contact with the bacteria, and free radicals have the ability to damage the cell membrane and make it porous which can ultimately lead to cell death (Tenzin et al., 2016). Silver is a soft acid, and there is a natural tendency of an acid to react with a base; in this case, a soft acid to react with a soft base. Another fact is that the deoxyribonucleic acid (DNA) has sulfur and phosphorus as its major components; AgNPs can act on these soft bases and destroy the DNA which would definitely lead to cell death (Masoud et al., 2016).

Antioxidant activity of silver nanoparticles

At 230 nm, absorbance of control was 0.432. The reduction in absorbance of hydrogen peroxide at 230 nm caused by the test samples were measured after 10 min. Experimental results are expressed as absorbance mean

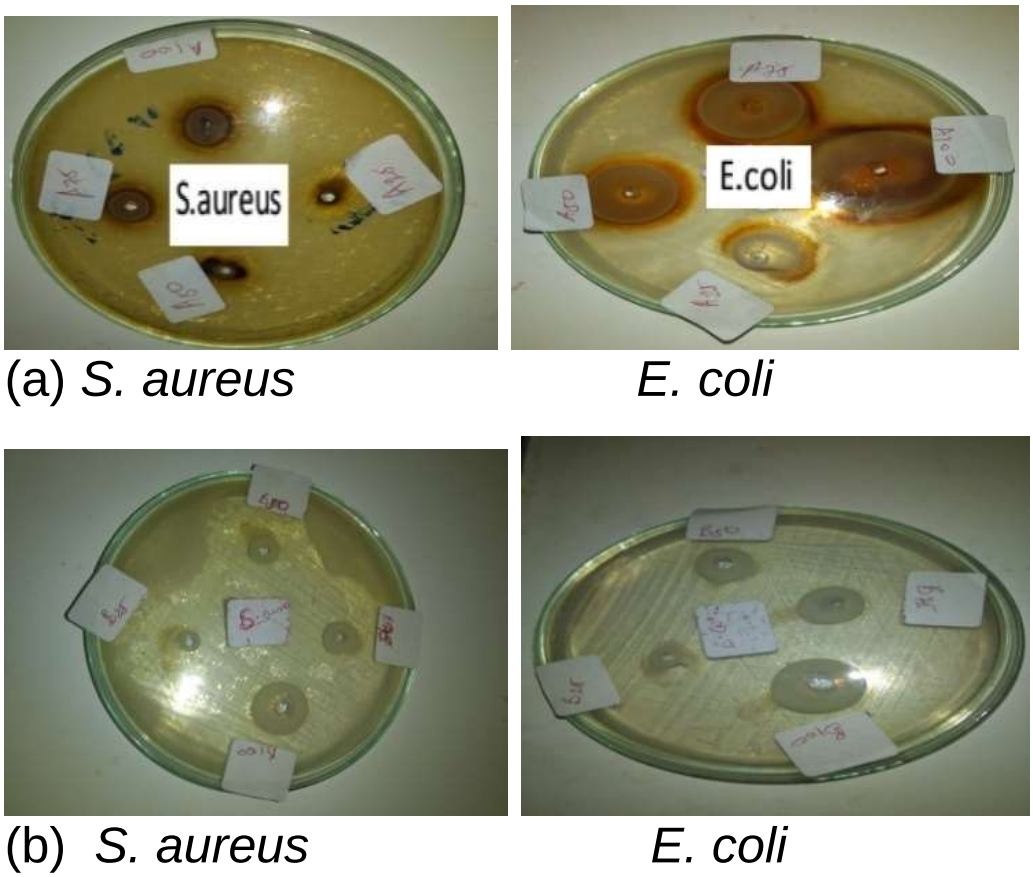

Figure 8. (a) Antibacterial testing with zone formation of AgNPs; **(b)** Silver nitrate against *S. aureus* and *E. coli.*

or % inhibition ± SD. The percentage of hydrogen peroxide scavenging by the test samples is calculated using the formula presented in the literature (Wilson et al., 2015) (Figure 9).

$$\% \text{ scavenged} = \frac{\text{absorbance of the control} - \text{absorbance of sample}}{\text{absorbance of the control}} \text{x100}$$

Hydrogen peroxide scavenging activity of AgNPs has showed maximum antioxidant activity observed (73.97 ±0.05%) in 50 µg/ml and minimum antioxidant activity observed (38.57 ± 0.07%) in 10 µg/ml. The radical scavenging activity is increased with the increasing concentrations of test samples.

It was reported that the percent of free radical scavenging activity of AgNPs is found to be high, due to its capability of good oxidant, electron loosing and capping agents present on AgNPs surface (Shahat and Assar, 2015). Hydrogen peroxide radical is not very reactive and it is a weak oxidizing agent; biologically, it acts as a toxicant to the cell by converting itself into hydroxyl radical in the presence of metal ions in living systems which results in initiation and propagation of lipid peroxidation (Shobana et al., 2016).

Conclusion

In the present study one pot synthesis, simple, clean, energy efficient, economically viable, and green approach has been established for the synthesis of AgNPs using non-toxic and renewable aqueous extract of *M. stenopetala* leaves as reducing, capping and stabilizing agents, and water as a solvent without using any harsh, synthetic reducing, capping and stabilizing agents.

It is found that the size of the AgNPs produced through bioreduction using aqueous extract of *M. stenopetala* leaves is strongly dependent on the synthesis parameters like heating time of extract, reaction time, silver nitrate concentration, and volume of aqueous extract of *M. stenopetala* leaves.

The findings of present study indicates that synthesis of AgNPs mediated by aqueous extract of *M. stenopetala* leaves had an efficient antibacterial, antioxidant activity and clearly indicate pharmaceutical and biomedical importance of AgNPs.

CONFLICT OF INTERESTS

The authors have not declared any conflict of interests.

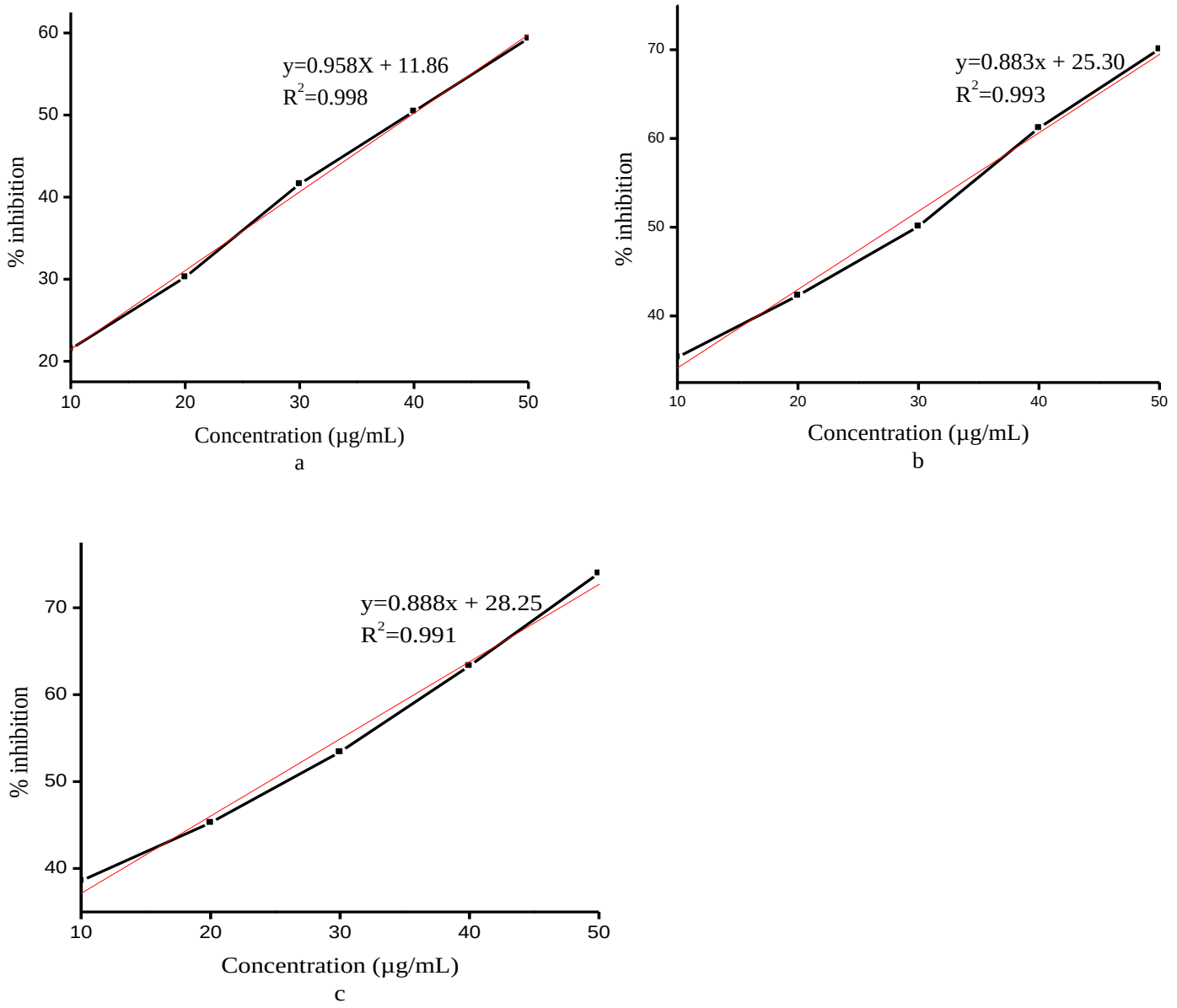

Figure 9. (a) Percentage inhibition of hydrogen peroxide scavenging activity of ascorbic acid. **(b)** Aqueous extract of *M. stenopetala* leaves, (c) Silver nanoparticles at different concentrations.

ACKNOWLEDGEMENT

The authors wish to thank Arba Minch College of Teachers Education, S.N.N.P.R, Ethiopia for the financial support towards the success of the research work.

REFERENCES

Abeer, AA (2016). Antibacterial effect of green synthesis silver nanoparticles against *Escherichia coli*. Res. J. Fish. Hydrobiol. 11(9):7-14.

Ahmed AE, Hafez AEH, Ismail FMA, Elsonbaty MS, Abbas HS, Eldin RAS (2015). Biosynthesis of silver nanoparticles by *Spirulina platensis* and *Nostoc sp. Glo.* Adv. Res. J. Microbiol. 4(4):36-49.

Balashanmugam P, Kalaichelvan TP (2015). Biosynthesis characterization of silver nanoparticles using *Cassia roxburghii* DC. aqueous extract, and coated on cotton cloth for effective antibacterial activity. Int. J. Nanomed. 10(1):87-97.

Basker GS (2016). Ecofriendly synthesis of silver nanoparticles *from Eichhornia crassipes.* Int. J. Curr. Res. Biosci. Plant Biol. 3(3):56-61.

Bonigala B, Usha KM, Vijayalakshmi M, Sambasiva R, Ravi VA, Poda S (2016). Green synthesis of silver nanoparticles from leaf extract of *Cascabela thevetia*, physicochemical characterization and antimicrobial activity. J. Pharm. Res. 10(6):410-418.

Bykkam S, Ahmadipour M, Narisngam S, Kalagadda RV, Chidurala CS (2015). Extensive studies on X-ray diffraction of green synthesized silver nanoparticles. Adv. Nanopart. 4(1):1-10.

Choudhary KM, Kataria J, Cameotra SS, Singh J (2016). A facile biomimetic preparation of highly stabilized silver nanoparticles derived from seed extract of *Vigna radiate* and evaluation of their antibacterial activity. Appl. Nanosci. 6(1):105-111.

Devadiga A, Shetty VK, Saidutta MB (2015). Timber industry waste-teak (*Tectona grandis* Linn.) leaf extract mediated synthesis of antibacterial silver nanoparticles. Int. Nano Lett. 5(1):205-214.

Fasasi AY, Mirjankar N, Fasasi A (2015). Fourier transform infrared spectroscopic analysis of protein secondary structures found in Egusi. Am. J. Appl. Ind. Chem. 1(1):1-4.

Gopalakrishnan V, Dhayalan M, Gandhi NN, Muniraj S (2016). Biosynthesis of silver nanoparticles using aqueous *Azadirachta indica* (neem) flower extract optimization, characterization and study of antimicrobial and antioxidant effects. Int. J. Innov. Res. Sci. Eng. Technol. 5(1):11-21.

Hassan AL, Elijah TA, Ojiefoh CO, Joseph O, Sunday OB, Olugbenga ED, Anuoluwapo AA (2016). Biosynthesis of silver nanoparticles using *Garcinia kola* and its antimicrobial potential. Afr. J. Pure Appl. Chem. 10(1):1-7.

Jassim NMA, Farhan AS, Dadoosh MR (2016). Green synthesis of silver nanoparticles using seed aqueous extract of *Abelmoschus esculentus* and study of their properties. Adv. Environ. Biol. 10(4):51-66.

Kekuda PRT, Raghavendra LH, Solomon T, Duressa D (2016). Antifungal and antiradical potential of *Moringa stenopetala* (Baker f.) Cufod (Moringaceae). J. Biosci. Agric. Res. 11(1):923-929.

Kumar B, Smita K, Cumbal L, Debut A, Camacho J, Gallegos HE, López G M C, Grijalva M, Angulo Y, Rosero G (2015). Pomosynthesis and biological activity of silver nanoparticles using *Passiflora tripartita* fruit extracts. Adv. Mater. Lett. 6(2):127-132.

Lakshman KD, Siva SS, Venkatesh P, Hepcy KD (2016). Green synthesis of silver nanoparticles using aerial parts extract of *Echinochloa colona* and their characterization. Eur. J. Pharm. Med. Res. 3(4):325-328.

Malathi R, Rajkumar K (2015). Synthesis of silver nanoparticles and its antimicrobial activity of *Coleus forskohlii*. World J. Pharm. Pharm. Sci. 4(9):673-678.

Marslin G, Selvakesavan KR, Franklin G, Sarmento B, Dias A (2015). Antimicrobial activity of cream incorporated with silver nanoparticles biosynthesized from *Withania somnifera.* Int. J. Nanomed. 10(1):5955-5963.

Masoud EA, Al-Hajry AM, Al-Marrani A (2016). Antibacterial activity of silver nanoparticles synthesized by *Sidr* (*Ziziphus spina- Christi*) leaf extract against pathogenic bacteria. Int. J. Curr. Microbiol. Appl. Sci. 5(4):226-236.

Mehmood A, Murtaza GG, Bhatti MT, Kausar R, Ahmed JM (2016). Biosynthesis, characterization and antimicrobial action of silver nanoparticles from root bark extract of *Berberis lycium* Royle. Pak. J. Pharm. Sci. 29(1):131-137.

Nagaonkar D, Rai M (2015). Sequentially reduced biogenic silver-gold nanoparticles with enhanced antimicrobial potential over silver and gold monometallic nanoparticles. Adv. Mater. Lett. 6(4):334-341.

Pak ZH, Abbaspour H, Karimi N, Fattahi A (2016). Eco-friendly synthesis and antimicrobial activity of silver nanoparticles using *Dracocephalum moldavica* seed extract. Appl. Sci. 6(69):1-10.

Parveen M, Ahmad F, Malla AM, Azaz S (2016). Microwave-assisted green synthesis of silver nanoparticles from *Fraxinus excelsior* leaf extract and its antioxidant assay. Appl. Nanosci. 6(1):267-276.

Premasudha P, Venkataramana M, Abirami M, Vanathi P, Krishna K, Rajendran R (2015).Biological synthesis and characterization of silver nanoparticles using *Eclipta alba* leaf extract and evaluation of its cytotoxic and antimicrobial potential. Bull. Mater. Sci. 38(4):965-973.

Priyanka S, Anupama D, Misna M, Jayan N, Reshma J, Reshma PR, Sana PA, Saranya KG, Vidya PV, Thomas L (2016). Phytochemical screening and biosynthesis of silver nanoparticles of selected medicinal plants used in traditional medicine. J. Med. Plants Stud. 4(4):1-5.

Raghasudha M (2016). Green synthesis of silver nanoparticles and study of catalytic activity. Int. J. Mod. Chem. Appl. Sci. 3(1):306-308.

Raghavendra LH, Kekuda PRT, Vijayananda NB, Duressa D, Solomon T (2016). Nutritive composition and antimicrobial activity of *Moringa stenopetala* (Baker f.) Cufod. J. Adv. Med. Pharm. Sci. 10(3):1-9.

Sadeenp S, Santhosh SA, Swamy KN, Suresh GS, Melo JS, Mallu P (2016). Biosynthesis of silver nanoparticles using *Convolvulus pluricaulis* leaf extract and assessment of their catalytic, electrocatalytic and phenol remediation properties. Adv. Mater. Lett. 7(5):383-389.

Saminathan K (2015). Herbal synthesis of silver nanoparticles using *Eclipta alba* and its antimicrobial activity. Int. J. Curr. Microbiol. Appl. Sci. 4(3):1092-1097.

Sangeetha R, Niranjan P, Dhanalakshmi N (2016). Characterization of silver nanoparticles synthesized using the extract of the Leaves of *Tridax procumbens.* Res. J. Med. Plant. 10(2):159-166.

Selvam GG, Sivakumar K (2015). Phycosynthesis of silver nanoparticles and photocatalytic degradation of methyl orange dye using silver (Ag) nanoparticles synthesized from *Hypnea musciformis* (Wulfen) J. V. Lamouroux. Appl. Nanosci. 5(1):617-622.

Shahat AS, Assar NH (2015). Biochemical and antimicrobial studies of biosynthesized silver nanoparticles using aqueous extract of *Myrtus communis L*. Ann. Biol. Res. 6(11):90-10.

Shobana G, Keerthana K, John NAA, Felicita SEA (2016). In vitro antioxidant potentials of aqueous extract of *Anacardium occidentale* L. World J. Pharm. Pharm. Sci. 5(1):1458-1467.

Sultana F, Barman J, Banik B, Saikia M (2015). A biological approach to synthesis of silver nanoparticles using aqueous leaf extract of *Houttuynia cordata* Thunb and comparative antioxidant study of plant extract and synthesized nanoparticles. Int. J. Mater. Biomater. Appl. 5(2):10-16.

Surya S, Kumar DG, Rajakumar R (2016). Green synthesis of silver nanoparticles from flower extract of *Hibiscus rosa-sinensis* and its antibacterial activity. Int. J. Innov. Res. Sci. Eng. Technol. 5(4):5242-5247.

Tenzin TN, Vishal G, Vitalis BM (2016). Silver nanoparticles: synthesis, mechanism of antimicrobial action, characterization, medical applications, and toxicity effects. J. Chem. Pharm. Res. 8(2):526-537.

Thampi N, Jeyadoss SV (2015a). Biogenic synthesis and characterization of silver nanoparticles using *Syzygium samarangense* (Wax Apple) leaves extract and their antibacterial activity. Int. J. Pharm. Tech. Res. 8(3):426-433.

Thampi N, Shalini VJ (2015b). Bio-prospecting the in-vitro antioxidant and anti-cancer activities of silver nanoparticles synthesized from the leaves of *Syzygium samarangense*. Int. J. Pharm. Pharm. Sci. 7(7):269-274.

Vastrad VJ, Goudar G (2016). Green synthesis and characterization of silver nanoparticles using leaf extract of *Tridax procumbens*. Orient. J. Chem. 32(3):1525-1530.

Wilson S, Cholan S, Vishnu U, Sannan M, Jananiya R, Vinodhini S, Manimegalai S, Rajeswari DV (2015). *In vitro* assessment of the efficacy of free-standing silver nanoparticles isolated from *Centella asiatica* against oxidative stress and its antidiabetic activity. Der Pharmacia Lettre. 7(12):194-205.

Wojtan PM, Liskiewicz KM, Depciuch J, Sadik O (2016). Green synthesis and antibacterial effects of aqueous colloidal solutions of silver nanoparticles using camomile terpenoids as a combined reducing and capping agent. Bioprocess. Biosyst. Eng. 39(1):1213-1223.

Zhang FX, Liu GZ, Shen W, Gurunathan S (2016). Silver Nanoparticles: Synthesis, Characterization, properties, applications, and therapeutic approaches. Int. J. Mol. Sci. 17(1534):1-34.